

## Three-Dimensional Models for Agonist and Antagonist Complexes with $\beta_2$ Adrenergic Receptor

Maria Kontoyianni,<sup>†,‡</sup> Carol DeWeese,<sup>†</sup> Julie E. Penzotti,<sup>†</sup> and Terry P. Lybrand<sup>\*,†</sup>

Molecular Bioengineering Program, Center for Bioengineering, Box 351750, University of Washington, Seattle, Washington 98195-1750, and ZymoGenetics Corporation, 1201 Eastlake Avenue E., Seattle, Washington 98102

Received March 27, 1996<sup>Ⓞ</sup>

Computer-modeling techniques have been used to generate docked complexes for a series of  $\beta$  adrenergic agonists and antagonists with a three-dimensional model of the  $\beta_2$  adrenergic receptor. For all ligands tested, it proved possible to dock low-energy conformers in the receptor model, with sensible electrostatic, steric, and hydrogen-bonding interactions, many of which are supported by experimental studies of the  $\beta_2$  receptor. Our results illustrate the power of molecular modeling techniques, when coupled with appropriate experimental methods and data, to investigate structure–function properties of integral membrane receptor proteins that cannot yet be studied by direct structural methods.

### Introduction

Integral membrane proteins often play a key role in signal transduction across membranes. The G-protein-coupled receptors (GPCR) represent a physiologically and pharmacologically important class of membrane-bound receptor proteins.<sup>1–3</sup> Several hundred proteins in organisms ranging from *Drosophila* to humans have been identified as members of this family. Nearly all GPCR identified to date appear to have a transmembrane domain composed of seven  $\alpha$ -helical segments, and they bind endogenous ligands ranging from epinephrine to small proteins. After the visual pigments, the adrenergic neurotransmitter receptors are probably the best-characterized GPCR.<sup>4</sup> Many of these receptors have become important pharmacological targets in treatment of a variety of disease states, due to their key role in control of numerous physiological processes. For example, many therapeutic agents utilized in treatment of asthma, hypertension, and various cardiac conditions exert their effects via interactions with adrenergic receptors. Detailed knowledge about the function of GPCR and their interactions with ligands would enhance significantly our understanding of cell-signaling processes and would also be of great value in development of improved therapeutic agents and treatment strategies for many disease states. Atomic-resolution structures of these proteins would contribute greatly to our understanding of receptor function and ligand interactions, but numerous technical problems prohibit the determination of atomic-resolution structures for most membrane proteins at present.

There is a growing body of indirect structural data available for some GPCR from various biophysical, ligand-binding, and site-directed mutagenesis experiments. In favorable cases, these indirect structural data may be used to construct crude three-dimensional (3D) models for GPCR. For example, numerous 3D models have been constructed for adrenergic receptors and other GPCR.<sup>5–17</sup> Many are based on the electron diffraction structure of bacteriorhodopsin,<sup>18</sup> although there is no significant sequence similarity observed

between bacteriorhodopsin and GPCR identified to date. The rationale for use of bacteriorhodopsin as a template structure for model building invokes general functional similarity between bacteriorhodopsin and rhodopsins from higher organisms and the fact that the rhodopsins are members of the G-protein-coupled receptor family. As has been pointed out previously, however, bacteriorhodopsin and the rhodopsins are not functional analogs.<sup>19</sup> Bacteriorhodopsin is a light-activated proton pump, while the rhodopsins are G-protein-coupled photoreceptors. The retinal chromophore is different in these two protein families (*all-trans*-retinal in bacteriorhodopsins and *11-cis*-retinal in rhodopsins), and the photoisomerization reactions differ as well. Recent modeling studies also raise questions regarding the validity of bacteriorhodopsin as a reference structure, on the basis of alternate sequence alignments or modeled ligand–receptor complexes.<sup>9,15,20</sup> In particular, these studies suggest that the helix bundle arrangement may be quite different from that observed in bacteriorhodopsin. As we have discussed in detail previously,<sup>21</sup> various hypotheses used to suggest sequence (and by implication, structural) homology between bacteriorhodopsins and GPCR generally propose either a gene duplication event for a small, primordial helix bundle protein,<sup>22</sup> or an exon-shuffling event that led to rearrangement of helices in the bundle, such that there is no clearly observable collinear sequence homology between the two families.<sup>20</sup> A detailed sequence comparison of all halobacterial retinal proteins and a number of G-protein-coupled receptors refutes both these hypotheses, however.<sup>23</sup> When the entire halobacterial retinal protein family is examined simultaneously with a large number of G-protein-coupled receptors, no data exist to support either hypothesis or any sequence homology between the two families. This suggests that either (1) the halobacterial retinal protein family (including bacteriorhodopsin) and the G-protein-coupled receptor family are the products of a highly divergent evolution from an ancient common ancestor or (2) these two protein families are the result of a convergent evolution event, i.e., evolutionary pressures have yielded two unrelated protein families that possess a similar tertiary structure (presumably because a seven-helix bundle is physically stable and functionally adaptable

\* Author to whom all correspondence should be addressed.

<sup>†</sup> University of Washington.

<sup>‡</sup> ZymoGenetics Corp.

<sup>Ⓞ</sup> Abstract published in *Advance ACS Abstracts*, October 1, 1996.

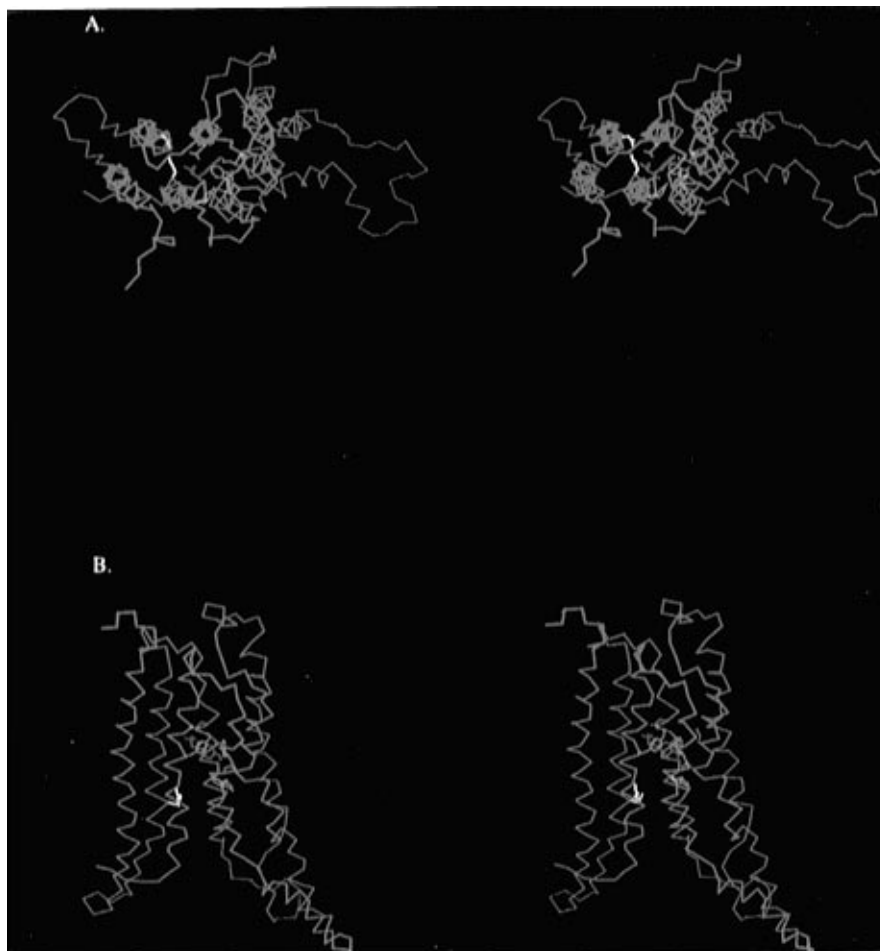


**Figure 1.** Stereoview of the complete  $\beta_2$  adrenergic receptor model complexed with epinephrine, after energy minimization and molecular dynamics relaxation.<sup>28</sup> The receptor backbone is shown in green, the ligand is blue, and side chains in the ligand binding site are displayed in red. A contact pair between Asp-79 and Asn-322 is highlighted in yellow: (A) top view and (B) side view. Note the marked kinking in helices at the sites of conserved proline residues.

in a lipid bilayer environment). While conclusions drawn from sequence analysis and modeling studies are not unequivocal, recent low-resolution electron diffraction structures for bovine and frog rhodopsins show clearly that there are significant differences in the transmembrane helix bundle-packing arrangements for rhodopsin versus bacteriorhodopsin.<sup>24,25</sup> The diffraction structure is not of sufficient resolution to evaluate the details of any particular model structure, but it does provide the first direct experimental evidence that bacteriorhodopsin is not the ideal template for G-protein-coupled receptor model-building studies. Therefore, we believe that it is essential that three-dimensional models for GPCR be constructed without any *a priori* assumption of similarity to bacteriorhodopsin.

We have reported previously the use of *de novo* model-building techniques to construct 3D models for  $\beta_2$  adrenergic receptor.<sup>9,21,26</sup> Our modeling procedure does not presume any sequence or structural relationship with bacteriorhodopsin. Instead, we started with two assumptions: (1) the transmembrane domain consists of seven  $\alpha$ -helical segments, as suggested by an assortment of secondary structure prediction methods and antipeptide antibody-mapping experiments,<sup>27</sup> and (2) the seven  $\alpha$ -helices are all oriented approximately perpendicular to the plane of the bilayer, in a continuous bundle arrangement as observed for bovine and frog rhodopsins.<sup>24,25</sup> Given these assumptions, the seven putative transmembrane  $\alpha$ -helical segments are first

constructed as idealized helices. These seven helices are then packed into bundle arrangements that segregate most polar residues in the bundle interior, with predominantly hydrophobic residues on the exterior (e.g., lipid-exposed) surface of the bundle. Multiple sequence alignments for a collection of GPCR provide important clues for helix orientation. These alignments reveal sides, or faces, in the transmembrane helices that possess the expected profile for a lipid-exposed surface; specifically, these lipid-exposed helix faces exhibit a complete lack of residue conservation, except that amino acid substitutions are restricted to hydrophobic residues. Unlike most other reported GPCR-modeling exercises, we also include extracellular and cytosolic loops in our model structures. While we can only generate physically sensible, but not unique, loop conformations in our models, inclusion of loops has proven to provide useful topological constraints in some cases. For example, some interhelical loops in  $\beta_2$  receptor and many other GPCR are quite short and dictate that the attached helices must pack next to each other in a bundle. Only those bundle arrangements that satisfy these general topological and physical property constraints and congregate residues shown to be important for ligand binding in a localized region of the bundle interior (i.e., form a putative ligand binding pocket) are retained for further consideration and model refinement. Topological and physical property constraints and constraints from site-directed mutagenesis

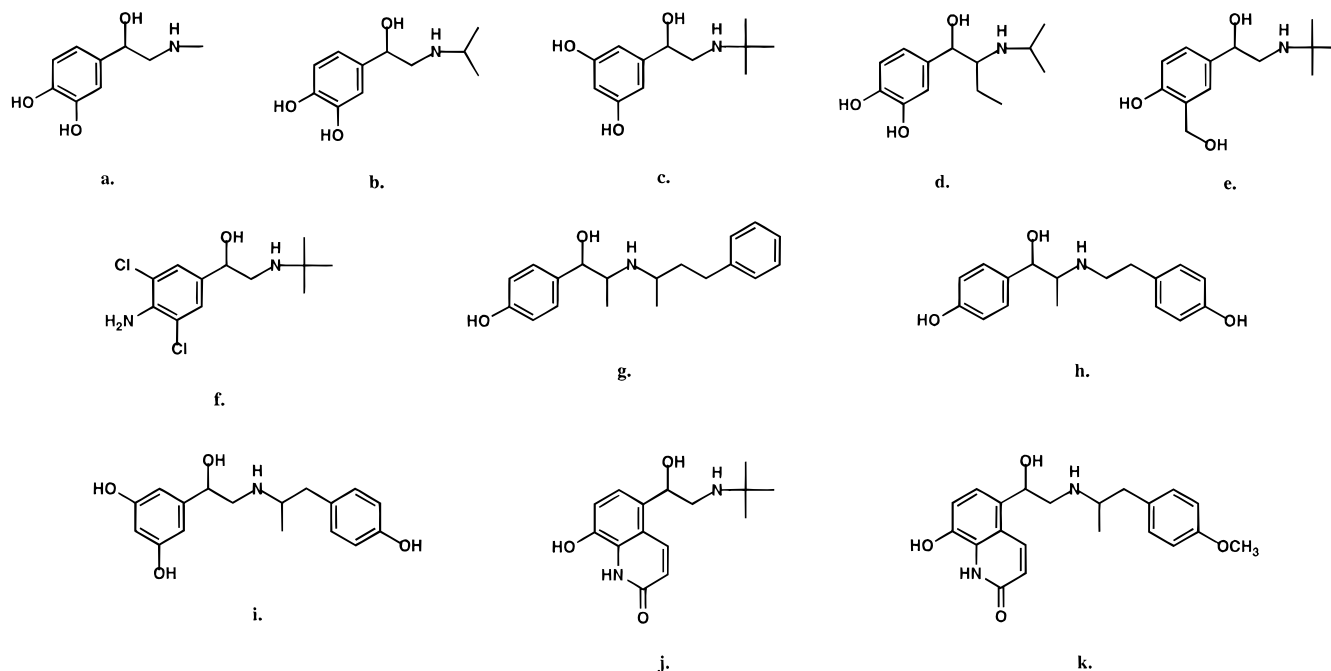


**Figure 2.**  $\beta$  Adrenergic agonists: (a) epinephrine {1-(3,4-dihydroxyphenyl)-2-(methylamino)ethanol}, (b) isoproterenol {1-(3,4-dihydroxyphenyl)-2-(isopropylamino)ethanol}, (c) terbutaline {2-(*tert*-butylamino)-1-(3,5-dihydroxyphenyl)ethanol}, (d) Isoetharine {1-(3,4-dihydroxyphenyl)-2-(isopropylamino)-1-butanol}, (e) albuterol {2-(*tert*-butylamino)-1-[4-hydroxy-3-(hydroxymethyl)phenyl]ethanol}, (f) clenbuterol {1-(4-amino-3,5-dichlorophenyl)-2-(*tert*-butylamino)ethanol}, (g) nylidrin {1-(4-hydroxyphenyl)-2-[(1-methyl-3-phenylpropyl)amino]-1-propanol}, (h) ritodrine {1-(4-hydroxyphenyl)-2-[[2-(4-hydroxyphenyl)ethyl]amino]-1-propanol}, (i) fenoterol {1-(3,5-dihydroxyphenyl)-2-[[4-(4-hydroxyphenyl)isopropyl]amino]ethanol}, (j) 8-hydroxy-5-[2-(*tert*-butylamino)-1-hydroxyethyl]-2-oxoquinoline, and (k) TA-2005 {8-hydroxy-5-[1-hydroxy-2-[[2-(4-methoxyphenyl)-1-methylethyl]amino]ethyl]-2-oxoquinoline}.

and biophysical studies enable us to reduce the number of helix bundle candidate structures from  $\sim 1500$  (the number of packing arrangement permutations for an approximately circular seven-helix bundle) to only 10–20 structures in most cases. These best-candidate structures are then subjected to energy minimization and molecular dynamics refinement,<sup>28</sup> yielding receptor models that display noticeably kinked and distorted helices packed in an array comparable to the rhodopsin projection map structures. For the  $\beta_2$  adrenergic receptor, there is adequate experimental data to permit us to reduce the helix bundle model candidates to two general classes: a clockwise and a counterclockwise helix bundle arrangement. Both general models are consistent with most available experimental data, although the clockwise model appears to better explain stereoselective ligand binding data.<sup>9</sup> The relaxed clockwise model with epinephrine docked in the putative binding site is shown in Figure 1.

To test further the reasonableness of our three-dimensional  $\beta_2$  receptor models, we have now performed ligand-docking studies for a wide range of  $\beta_2$  ligands that vary in size and functional group substitution (Figures 2 and 3). If our initial 3D receptor models are reasonable, they should accommodate a wide range of ligands *with little or no adjustment of the receptor models*. We present here the results of these ligand-docking exercises.

## Results and Discussion

Since all ligands share at least some common features, we will not present a detailed analysis of each complex here. Instead, we will describe features common to all ligand complexes studied and then present

in detail those ligand complexes that are representative of a group or else unique in some key aspects.

It proved possible to dock all ligands shown in Figures 2 and 3 in the  $\beta_2$  receptor model with energetically reasonable conformations. All share some common features—e.g., each ligand forms a charge-pair-reinforced hydrogen bond between protonated amine and Asp-113 from transmembrane helix 3 of the receptor, as expected from previous modeling work<sup>9</sup> and experimental studies.<sup>29</sup> The chromophore of each ligand stacks between Trp-286 and Phe-290 from helix 6 as reported previously.<sup>9</sup> The presence of Gly-315 in helix 7 also appears to be important. Our models suggest that a larger residue at this position in helix 7 would introduce significant steric restrictions in the ligand binding pocket. This glycine is highly conserved among GPCR that exhibit measurable binding for catechol ligands (e.g., adrenergic, dopaminergic, and serotonergic receptors). The  $\beta_2$  receptor exhibits rather dramatic stereoselectivity for chiral ligands, and the preferred stereoisomer for typical agonists and antagonists is shown in Figure 4. All ligands docked in our clockwise helix-bundle model form a good hydrogen bond with Ser-319 or an alternate residue from helix 7. Ligands docked in the counterclockwise helix-bundle model form a hydrogen bond with Thr-164 from helix 4. Most other features are particular to either agonists or antagonists, and a number of ligands display certain unique receptor site interactions.

**Agonists.** Each agonist studied possesses one or two hydroxyl groups on the aromatic ring system capable of forming hydrogen bonds with conserved serines 204 and/or 207 in helix 5. Experimental data suggest that the *p*-hydroxy group of catechols forms a hydrogen bond with Ser-207, while the *m*-hydroxy group interacts with

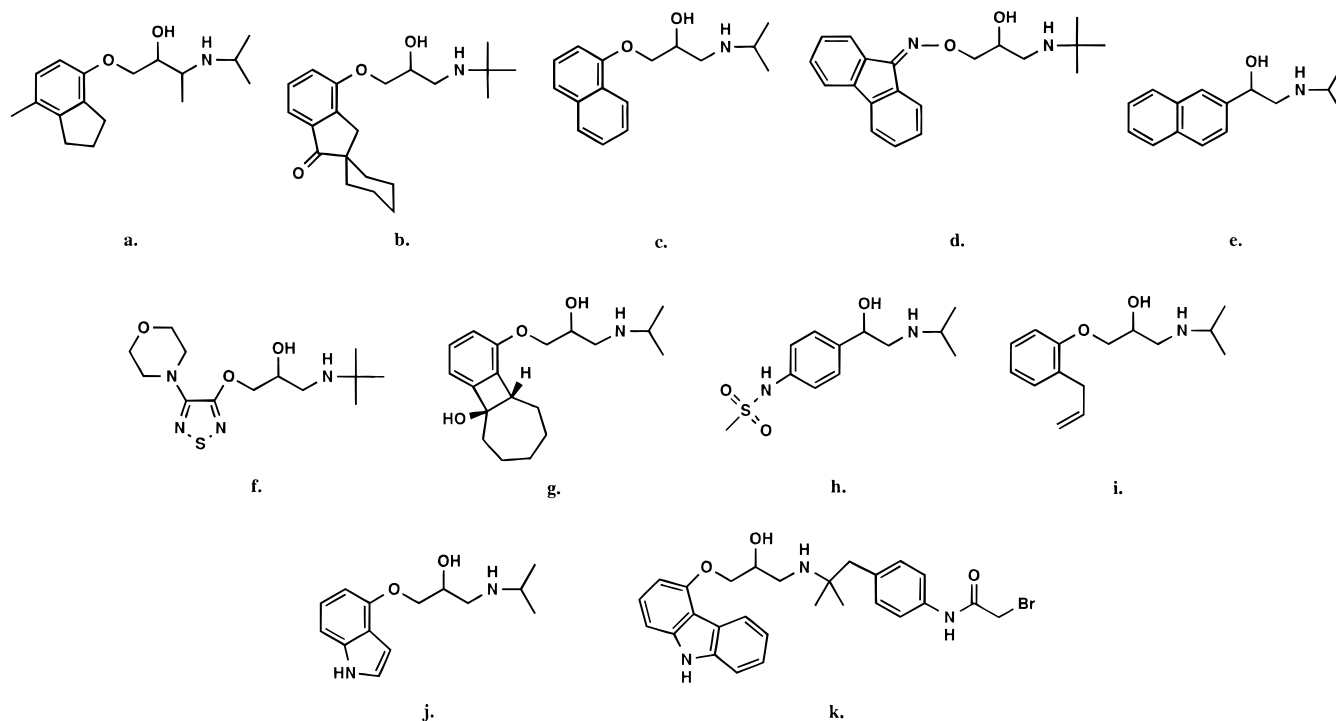


**Figure 3.**  $\beta$  Adrenergic antagonists: (a) ICI-118,551 {erythro-1-[(7-methylindan-4-yl)oxy]-3-(isopropylamino)-2-butanol}, (b) spiroindolol {4'-[3-(*tert*-butylamino)-2-hydroxypropoxy]spiro[cyclohexane-1,2'-indan]-1'-one}, (c) Propranolol {1-(isopropylamino)-3-(1-naphthoxy)-2-propanol}, (d) IPS-339 {9-[3-(*tert*-butylamino)-2-hydroxypropoxy]oximino]fluorene}, (e) pronethalol {1-(2'-naphthyl)-2-(isopropylamino)ethanol}, (f) timolol {1-(*tert*-butylamino)-3-[(4-morpholino-1,2,5-thiadiazol-3-yl)oxy]-2-propanol}, (g) 1-[3-(isopropylamino)-2-hydroxypropoxy]-4b,6,7,8,9,9a-hexahydro-5H-benzo[3,4]cyclobuta[1,2]cyclohepten-4b-ol, (h) sotalolol {*N*-[4-[1-hydroxy-2-(isopropylamino)ethyl]phenyl]methanesulfonamide} (i) alprenolol {1-(isopropylamino)-3-[2-(2-propenyl)phenoxy]-2-propanol}, (j) pindolol {1-(1H-indol-4-yloxy)-3-(isopropylamino)-2-propanol}, and (k) [*p*-(bromoacetamido)benzyl]carazolol {4-[2-hydroxy-3-[[2-[4-bromoacetamido]phenyl]-1,1-dimethylethyl]amino]propoxy]carbazole}.

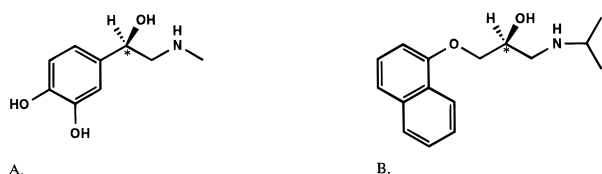


**Figure 4.** Preferred stereoisomers for  $\beta_2$  adrenergic agonists and antagonists: (A) (*R*)-epinephrine, a typical catecholamine agonist, and (B) (*S*)-propranolol, a typical antagonist in the phenylpropanolamine series. Note that the absolute configuration of each molecule is the same.

Ser-204.<sup>30</sup> Most agonists that possess only one hydroxyl group have it substituted in the *para* position of the aromatic ring (see Figure 2); these ligands invariably formed a hydrogen bond with Ser-207 in our relaxed structures. Interestingly, in a previous MD simulation for an epinephrine–receptor–bilayer complex, it appears that the *p*-OH/Ser-207 hydrogen bond is much more stable than hydrogen bonds involving Ser-204.<sup>28</sup> These specific hydrogen bonds for *m*- and *p*-hydroxyl groups, together with the charge interaction between the protonated amine and Asp-113, form a three-point attachment that greatly restricts the rotational freedom of catecholamine ligands in the receptor binding pocket.

For smaller agonists (e.g., terbutaline, Figure 2c; isoetharine, Figure 2d), the ligand–receptor interactions are quite similar to those for epinephrine reported previously.<sup>9</sup> In addition to common features listed above, the *N*-alkyl substituents from these ligands (-CH<sub>3</sub>, -CH(CH<sub>3</sub>)<sub>2</sub>, -C(CH<sub>3</sub>)<sub>3</sub>) interact with Val-117 in helix 3 and neighboring hydrophobic residues. For the bulky *tert*-butyl group in terbutaline, the Val-117 side chain had to be rotated to a new conformation to avoid

serious steric overlap with the ligand. Among the small agonists, isoetharine was probably the most difficult to dock because the ethyl group in the  $\alpha$ -position of the side chain presents additional possible steric conflicts. However, all the small agonists can be docked in low-energy conformations (only ~1–3 kcal/mol above the global minimum found in systematic search). A typical complex with the *R* isomer of epinephrine is shown in Figures 5 and 6.

The larger agonists (e.g., ritodrine, Figure 2h) presented greater steric challenges during docking exercises. When ionic and hydrogen bond contacts described above are imposed, and the chromophore is stacked between Trp-286 and Phe-290, the large 2-phenylethyl *N*-substituent must lie in a pocket formed by residues from helices 2 and 7. In this orientation, the aromatic ring of the *N*-substituent stacks nicely with Met-40 from helix 1 and Phe-89 from helix 2, the ethyl fragment packs against Val-117 from helix 3, and the *p*-OH group of the phenethyl substituent forms a hydrogen bond with Asn-318 from helix 7, as seen in Figures 7 and 8. Interestingly, there is some experimental data to support a role for Asn-318 in agonist interactions.<sup>31</sup> In the case of ritodrine and related compounds, a slightly higher energy conformer (~5 kcal/mol above the global minimum) fits best in the binding site. Most other large agonists have considerable structural similarity with ritodrine, and their binding interactions with the receptor are comparable. The variations in methyl substitution patterns around the amine group in compounds **2g–i,k** do not alter substantially the nature of the ligand–receptor complexes because the ethyl chains are reasonably flexible (our models predict that substituents

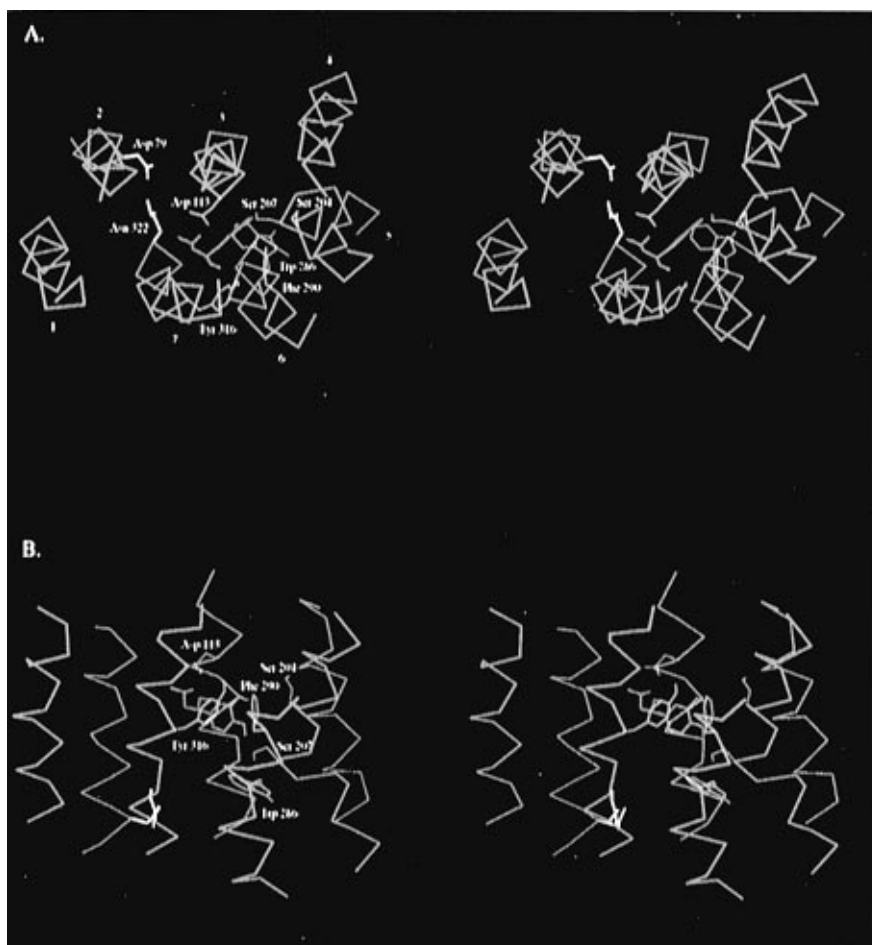


**Figure 5.** Stereoviews of the (*R*)-epinephrine complex with the clockwise  $\beta_2$  receptor model after limited energy minimization and molecular dynamics refinement. These images are stereoviews of a thin slice through the center region of the seven-helix bundle that comprises the ligand binding site. The  $\alpha$ -carbon backbone is shown in green, the ligand is colored blue, and key binding site residues are displayed in red and include Asp-113 in helix 3, Ser-204 and Ser-207 in helix 5, Trp-286 and Phe-290 in helix 6, and Tyr-316 in helix 7. The contact pair formed between Asp-79 from helix 2 and Asn-322 from helix 7 is highlighted in yellow. (A) Top view from the extracellular side: Helices 1, 3, 5, and 7 project into the plane of the figure (amino terminus to carboxy terminus), while helices 2, 4, and 6 project out of the page in the amino to carboxy direction. (B) Side view. Figures 5, 7, 9, 11, and 13 were generated with the Molsript program.<sup>54</sup>

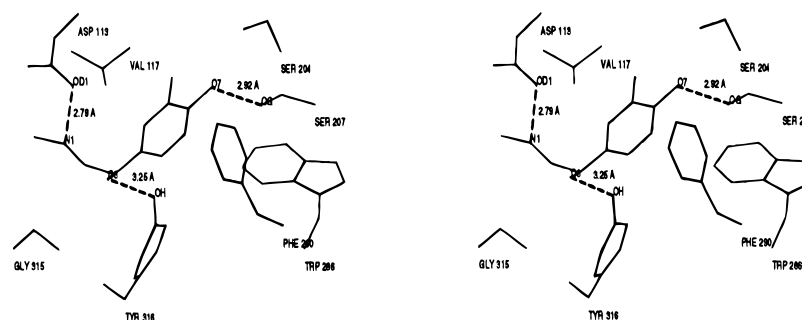


**Figure 6.** Detailed stereoview of the epinephrine binding site. Only key binding site residue side chains are displayed (Asp-113, Ser-204, Ser-207, Trp-286, Phe-290, Gly-315, and Tyr-316), and key ligand-receptor contact distances are highlighted with dashed lines. The orientation is similar to that shown in Figure 5A.

larger than a methyl group would likely produce more significant steric clashes with receptor side chains, altering the docked ligand conformation substantially and/or lowering binding affinity due to unfavorable van der Waals interactions).

In general, it was rather easy and straightforward to dock all the agonists in the receptor models with low-energy conformations. The antagonists presented greater challenges, due to a generally much larger size of these compounds (Figure 3).

**Antagonists.** Unlike the agonists, none of the an-

tagonists possess suitable functional groups on the chromophore to form hydrogen bonds with serines in helix 5. As we observed previously, this is one key feature that is consistently different for agonists versus antagonists and is likely significant.<sup>9</sup> Smaller antagonists like propranolol (Figure 3c) and pronethalol (Figure 3e) can be docked rather easily in the receptor models. As with the smaller agonists, the *N*-alkyl substituents are positioned to form favorable van der Waals interactions with Val-117 and other nearby hydrophobic residues. Propranolol forms a complex

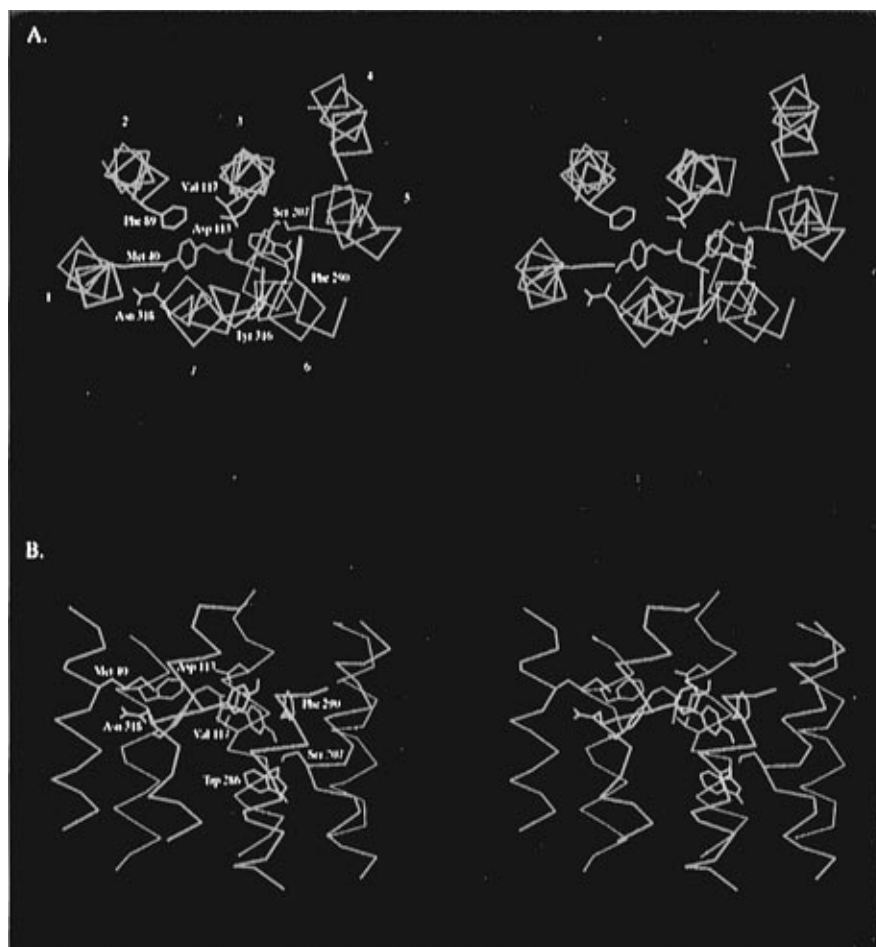


**Figure 7.** Stereoviews of the ritodrine complex with the clockwise  $\beta_2$  receptor model after limited energy minimization and molecular dynamics refinement. The orientation and color coding is as listed for Figure 5. Key active site residues, shown in red, include Met-40 from helix 1, Phe-89 in helix 2, Asp-113 and Val-117 in helix 3, Ser-207 from helix 5, Trp-286 and Phe-290 in helix 6, and Tyr-316 and Asn-318 from helix 7: (A) top view and (B) side view.

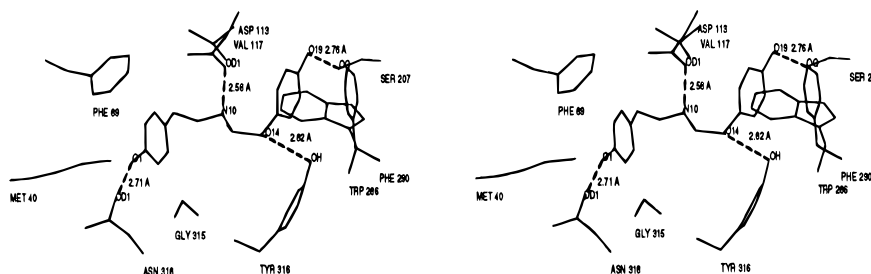


**Figure 8.** Detailed stereoview of the ritodrine binding site. Only key binding site residue side chains are displayed (Met-40, Phe-89, Asp-113, Val-117, Ser-207, Trp-286, Phe-290, Gly-315, Tyr-316, and Asn-318), with key ligand-receptor contacts highlighted by dashed lines. The orientation is similar to that shown in Figure 7A.

typical of the small molecule antagonists and is shown in Figures 9 and 10. The propranolol chromophore stacks between Trp-286 and Phe-290 and forms additional contacts with Cys-116 from helix 3 and Tyr-316 from helix 7. The *N*-isopropyl substituent interacts with Met-40 from helix 1, Phe-89 from helix 2, and Val-117 from helix 3. Note that for propranolol (and all other antagonists in the phenylpropanolamine series), the *S* isomer is the preferred stereoisomer and that (*S*)-propranolol has the same absolute configuration at the chiral side chain carbon as does (*R*)-epinephrine (Figure 4).

Several antagonists have quite bulky chromophores, and spirodolo (Figure 3b) is perhaps most dramatic. This compound has a large chromophore with an attached cyclohexyl ring that projects into a hydrophobic

pocket formed by residues in helices 3 and 4. Cys-116 and Val-117 from helix 3, Trp-286 and Phe-290 from helix 6, and Tyr-316 from helix 7 form the primary favorable contacts with the cyclohexyl ring and chromophore, while the *tert*-butyl substituent interacts with Met-40 from helix 1, Val-86 and Phe-89 from helix 2, and Val-117 from helix 3, as shown in Figures 11 and 12.

With the exception of carazolol, we were able to dock the lowest-energy conformer of each antagonist into the binding site with little or no receptor structural adjustments. Carazolol is by far the largest ligand we have attempted to dock, and the best fit to date requires a conformer that is  $\sim 7$ – $8$  kcal/mol above the global minimum found in the systematic search. While this energy threshold is somewhat higher than we have

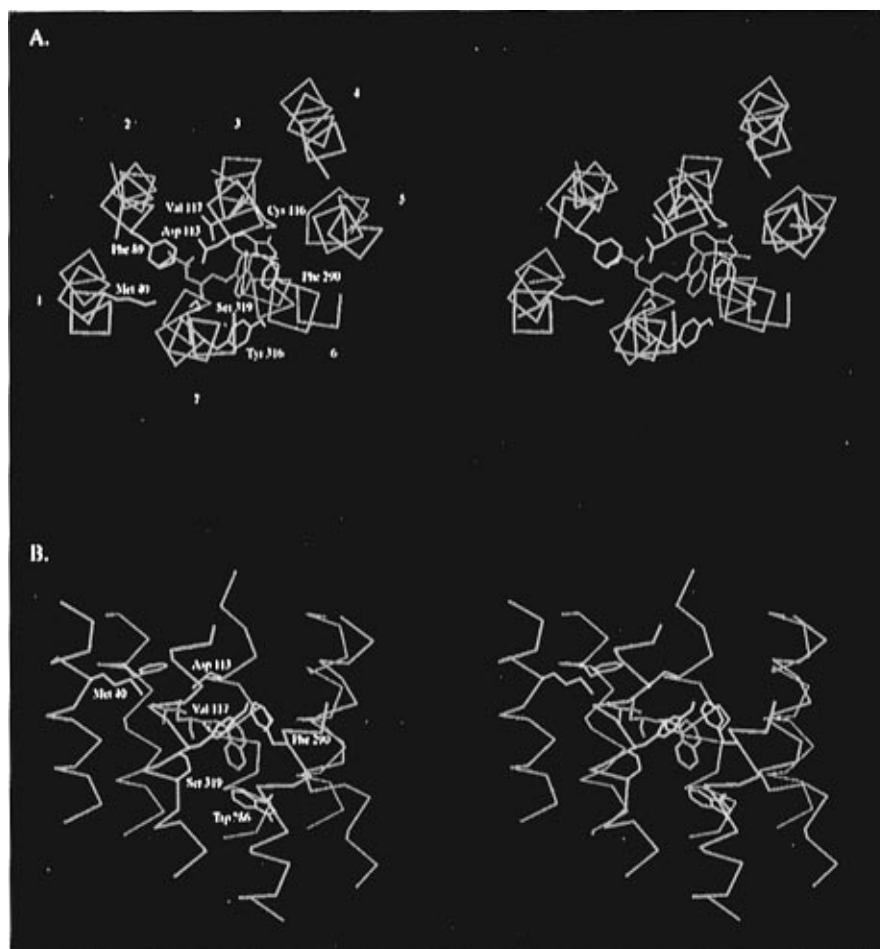


**Figure 9.** Stereoviews of the propranolol complex with the clockwise  $\beta_2$  receptor model after limited energy minimization and molecular dynamics refinement. Orientations and color schemes are as described for Figure 5. Key binding site residues include Met-40 from helix 1, Phe-89 in helix 2, Asp-113, Cys-116, and Val-117 in helix 3, Trp-286 and Phe-290 in helix 6, and Tyr-316 and Ser-319 in helix 7: (A) top view and (B) side view.

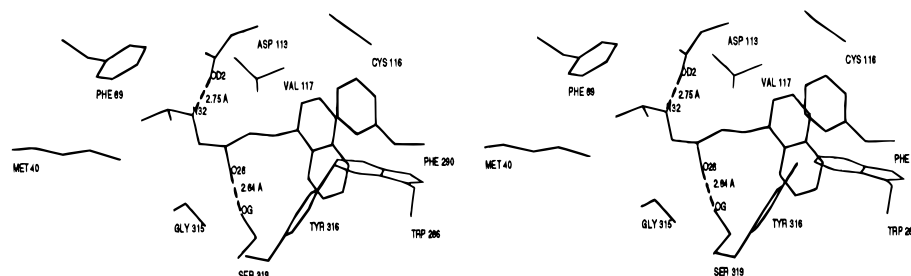


**Figure 10.** Detailed stereoview of the propranolol binding site. Only key binding site residue side chains are displayed (Met-40, Phe-89, Asp-113, Cys-116, Val-117, Trp-286, Phe-290, Gly-315, Tyr-316, and Ser-319), with key ligand-receptor contacts highlighted by dashed lines. The orientation is similar to that shown in Figure 9A.

permitted for all other ligands, it is still within the guidelines employed by others in conformational search and docking procedures.<sup>32</sup> The final carazolol-receptor complex is quite similar to the docked structure reported previously.<sup>9</sup> The ionic interaction is formed with Asp-113, and the chromophore stacks between Trp-286 and Phe-290. The large *p*-(bromoacetamido)benzyl substituent on the nitrogen projects into a pocket formed by helices 2 and 7, similarly to ritodrine and other large agonists. The benzyl aromatic ring stacks with Met-36 and Met-40 from helix 1 and Phe-89 from helix 2, and the bromoacetamido group is positioned to be susceptible to nucleophilic attack by Ser-92 or His-93 in helix 2, as documented previously in experimental studies.<sup>33</sup> The refined carazolol complex is shown in Figures 13 and 14. It should be noted that this docking orientation

is the only obvious possibility for carazolol in our models. Only the Asp-113/ligand amine interaction and ligand chromophore stacking with Trp-286 and Phe-290 were imposed as constraints in the docking exercises. The placement of the alkylating side chain near Ser-92 and His-93 is essentially dictated by the clockwise helix-bundle model and the criteria listed above.

**Manual versus Automated Docking.** Since we have good experimental data concerning some key ligand-receptor interactions, we can use this information as constraints when we construct ligand-receptor complex models. In fact, some constraint information is necessary to make a manual docking exercise feasible. Without constraint information, there are generally too many viable docking options to consider and evaluate with manual docking techniques. However, manual

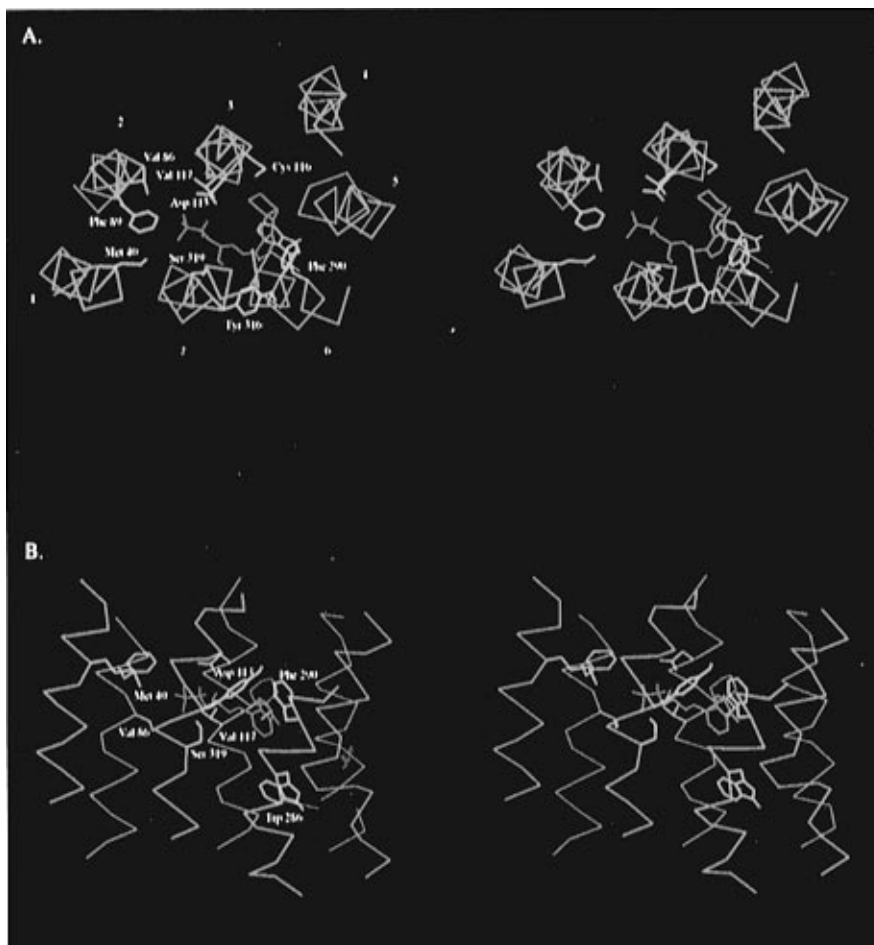


**Figure 11.** Stereoviews of the spirodrolol complex with the clockwise  $\beta_2$  receptor model after limited energy minimization and molecular dynamics refinement. Orientations and color schemes are as described for Figure 5. Key binding site residues displayed include Met-40 from helix 1, Val-86 and Phe-89 in helix 2, Asp-113, Cys-116, and Val-117 in helix 3, Trp-286 and Phe-290 in helix 6, and Tyr-316 and Ser-319 in helix 7: (A) top view and (B) side view.

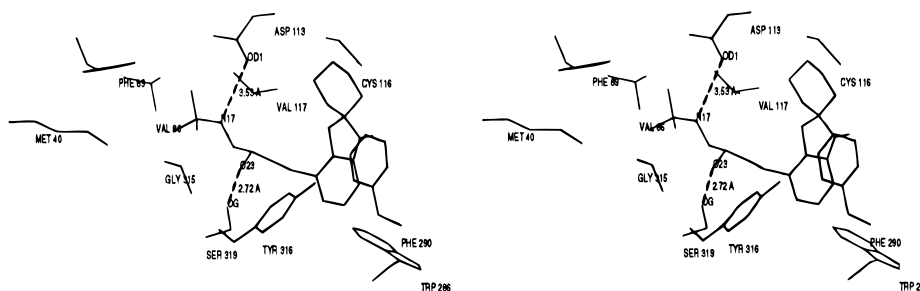


**Figure 12.** Detailed stereoview of the spirodrolol binding site. Only key binding site residue side chains are displayed (Met-40, Val-86, Phe-89, Asp-113, Cys-116, Val-117, Trp-286, Phe-290, Gly-315, Tyr-316, and Ser-319), with key ligand-receptor contacts highlighted by dashed lines. The orientation is similar to that shown in Figure 11A.

model-building exercises always require some subjective decisions, and there is the danger that personal biases, ambiguous experimental data, or inappropriate interpretation of experimental data could corrupt the manual ligand-docking exercises. To address these issues, we have used an automated docking procedure to determine the "best" binding locations and orientations for several ligands and compared these results with our manually constructed complexes.

We employed the automated ligand-docking program DOCK<sup>34</sup> to generate receptor complexes with epinephrine (Figure 2a), ritodrine (Figure 2h), and spirodrolol (Figure 3b), and details of these docking exercises are reported elsewhere;<sup>35</sup> 6–10 top-scoring docked complexes were examined carefully for each ligand. In each

case, the best DOCK-generated complexes (as determined by both simple steric and potential energy function scores) were structurally indistinguishable from our manually constructed complexes. DOCK-generated complexes that exhibit an alternate binding model (i.e., a binding site that is not located between Asp-113 from helix 3 and Phe-290 from helix 6, or a model with ligand orientations distinctly different from any we developed in manual docking exercises) score much worse than the best DOCK-generated models. These results from the automated docking calculations give us confidence that our manually generated models are not influenced unduly by personal biases or failure to consider alternate options.

**General Features.** We have also performed a



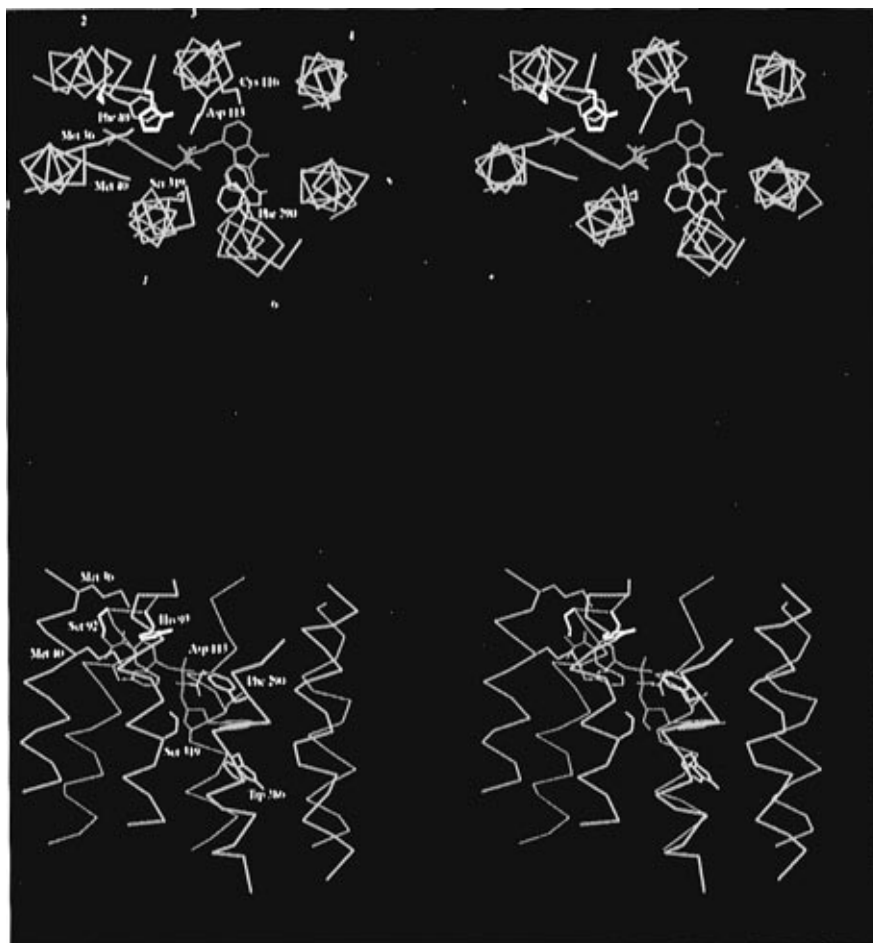


**Figure 13.** [(Bromoacetamido)benzyl]carazolol complex with the clockwise  $\beta_2$  receptor model after limited energy minimization and molecular dynamics refinement. The orientation and color schemes are as described in Figure 5. Key binding pocket residues include Met-36 and Met-40 from helix 1, Phe-89 in helix 2, Asp-113 and Cys-116 from helix 3, Trp-286 and Phe-290 in helix 6, and Ser-319 in helix 7. Also shown in yellow are Ser-92 and His-93 from helix 2. These residues are the sites of alkylation for the bromoacetamido group, which sits directly adjacent to these two residues in the model: (top) top view and (bottom) side view.

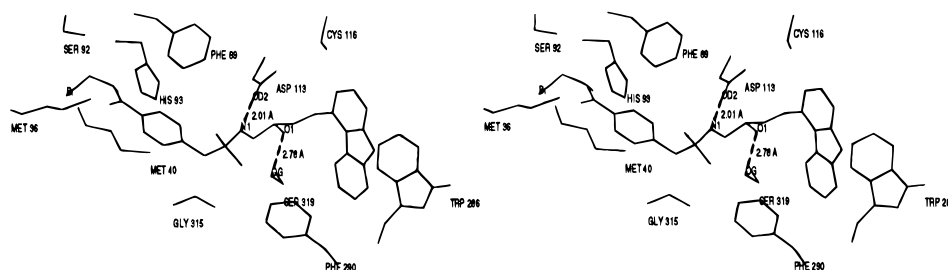


**Figure 14.** Detailed stereoview of the carazolol binding site. Only key binding site residue side chains are displayed (Met-36, Met-40, Phe-89, Ser-92, His-93, Asp-113, Cys-116, Trp-286, Phe-290, Gly-315, and Ser-319), with key ligand-receptor contacts highlighted by dashed lines. The orientation is similar to that shown in Figure 13, top.

detailed comparison of the clockwise and counterclockwise (i.e., bacteriorhodopsin-like) helix-bundle models for the  $\beta_2$  receptor with several ligands. As reported previously,<sup>26,28</sup> both models satisfy most physical property evaluation criteria equally well. Most ligand-receptor side chain interactions are also comparable in the two models. For example, the counterion/Asp-113 interaction, chromophore stacking, and specific catechol hydrogen bonds with serines 204 and 207 are common to both models. The most significant difference in these two models involves the receptor hydrogen bond partner for the hydroxyl attached to the chiral side chain carbon in each ligand. This interaction is significant because it is probably the principal determinant for stereoselective binding of ligands. The three-point attachment

described above for catecholamines, involving the protonated amine interaction with Asp-113 and specific hydrogen bonds between the *m*-hydroxy group and Ser-204 and the *p*-hydroxy group and Ser-207, eliminates the possibility of much rotational and/or translational freedom for the ligand in the binding pocket. Thus, the three-point attachment model determines the orientation of the side chain hydroxyl group in the ligand binding site and greatly restricts the number of possible hydrogen-bonding partners from the receptor. In the clockwise models, the side chain hydroxyl projects toward helix 7, and the best candidate hydrogen bond partner is Ser-319 or Tyr-316. In the counterclockwise models, the side chain hydroxyl projects toward helix 4, and the most probable side chain partner is Ser-161,

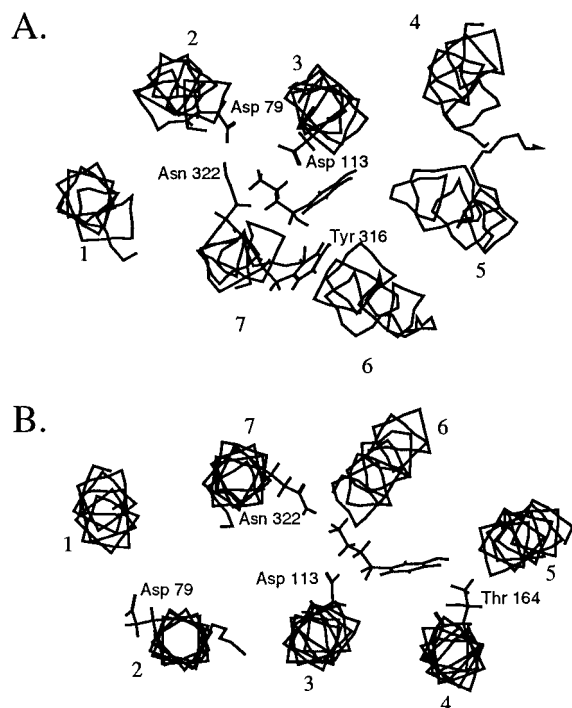


**Figure 15.** Clockwise and counterclockwise models for the  $\beta_2$  adrenergic receptor helix bundles after structural relaxation with energy minimization and molecular dynamics. Each bundle is viewed from the extracellular surface, and all extracellular and cytosolic loops have been removed for clarity. Helices are numbered consecutively. (A) Clockwise model with a docked (*R*)-epinephrine molecule: Asp-113 from helix 3 and Tyr-316 from helix 7 are shown as key anchor and stereoselective hydrogen-bonding residues in this model. The Asp-79/Asn-322 contact pair is clearly evident in the clockwise model. (B) Counterclockwise model: Asp-113 from helix 3 and Thr-164 from helix 4 are shown as the principal anchor and stereoselective hydrogen-bonding residues, respectively, in this model. Asp-79 and Asn-322 do not form a contact pair in the counterclockwise model, as seen clearly here.

Thr-164, or Ser-165 (Figure 15). Previous experimental studies have shown that mutation of Ser-161 to alanine has no effect on ligand binding,<sup>30</sup> and multiple sequence alignments show that Thr-164 is conserved only in  $\beta_2$ , but not  $\beta_1$ ,  $\beta_3$ , or  $\alpha$  adrenergic receptors, so these residues are not good candidates for the stereoselective hydrogen bond partner. Attempts to mutate Ser-165 to alanine yielded a  $\beta_2$  receptor that does not appear to fold and insert into the membrane.<sup>30</sup> There is some experimental data to suggest that mutation of Ser-319 to alanine diminishes agonist binding affinity.<sup>30</sup> However, this mutation does not appear to affect antagonist binding, and there is no evidence that it has any profound effect on stereoselectivity. Recent molecular dynamics simulations for epinephrine and propranolol receptor complexes in an explicit lipid bilayer model<sup>28</sup> suggest that Tyr-316 from helix 7 might form a strong, stable hydrogen bond with the epinephrine side chain hydroxyl, as shown in Figures 5 and 6. During these simulations, we observed that the hydroxyl/Ser-319 hydrogen bond in the original clockwise model broke and was replaced quickly by a good hydrogen bond with Tyr-316 that persisted for the duration of the simulations. This tyrosine is located approximately one turn earlier in the helix and can easily swing into position to form a hydrogen bond with the ligands. Recent experimental studies to probe residues from helix 4 indicate that

mutation of Thr-164 to alanine reduces the stereoselective binding preference for some agonists and antagonists, with no measurable effect on others.<sup>36</sup> Finally, a recent (counterclockwise)  $\beta_2$  receptor model based on the low-resolution bovine rhodopsin projection map suggests that Asn-293 from helix 6 functions as the stereoselective hydrogen bond partner.<sup>16</sup> Both our clockwise and counterclockwise models indicate that Asn-293 does indeed project into the proposed ligand binding pocket, although in our models it is too far away from the ligands to form a good hydrogen bond. However, Asn-293 is conserved only in  $\beta$  adrenergic receptors and is generally a nonpolar residue in all other adrenergic receptors. If the incorrect stereoisomer for any ligand is docked so as to maintain the charge-pair interaction between the protonated amine and Asp-113 and the side chain hydroxyl hydrogen bonds with residues in helix 7 (clockwise model) or helix 4 (counterclockwise model), the specific catechol hydrogen bonds with serines 204 and 207 are swapped and generally degraded (poorer geometries and/or hydrogen-bonding distances). This is in direct conflict with the experimental results<sup>30</sup> and forms the basis of our hypothesis for stereoselectivity in the receptor models.

In an attempt to gain some additional insight into the nature of ligand–receptor contacts and the stereoselective hydrogen-bonding interaction in particular, we have used multiple-sequence alignments for a large collection of adrenergic and other amine neurotransmitter receptors, some of which are shown in Figure 16. Given the assumption that  $\alpha_1$ ,  $\alpha_2$ , and all  $\beta$  adrenergic receptors have similar ligand receptor sites,<sup>16</sup> we hoped to derive additional clues about the nature of ligand–receptor interactions from this analysis. As can be seen in Figure 16, the alignment appears to rule out certain residues as candidates for the stereoselective hydrogen bond partner. In particular, Asn-293 from helix 6 is not conserved in  $\alpha$  adrenergic receptors, and Thr-164 from helix 4 is not even conserved among all  $\beta$  adrenergic receptors. In contrast, residues like Ser-165 from helix 4 or Ser-319 from helix 7 are too highly conserved, that is, these two positions are highly conserved in many GPCR (data not shown), including other amine neurotransmitter receptors, peptide receptors, etc., that do not bind ligands which require a stereoselective hydrogen–bonding interaction. This high degree of conservation for Ser-165 and Ser-319 in many diverse GPCR strongly suggests that they play an important structural role in the GPCR superfamily. The experimental data cited above for mutation of Ser-165 and Ser-319 in the  $\beta_2$  receptor are consistent with this hypothesis.

The multiple-sequence alignments do not pinpoint a single residue as a clear, best candidate for the stereoselective hydrogen-bonding partner. However, other interesting and exciting patterns are observed. A number of residues proposed to comprise the binding pocket and interact with ligands in our clockwise  $\beta_2$  receptor models exhibit systematic variations among adrenergic and other amine neurotransmitter receptors. For example, position 293 in the  $\beta_2$  receptor (and the corresponding position in all other adrenergic receptors) is always asparagine in  $\beta$  receptors, tyrosine in  $\alpha_2$  receptors, and specific hydrophobic residues in different  $\alpha_1$  receptor subtypes. Extension of this analysis reveals other positions that appear to display systematic se-

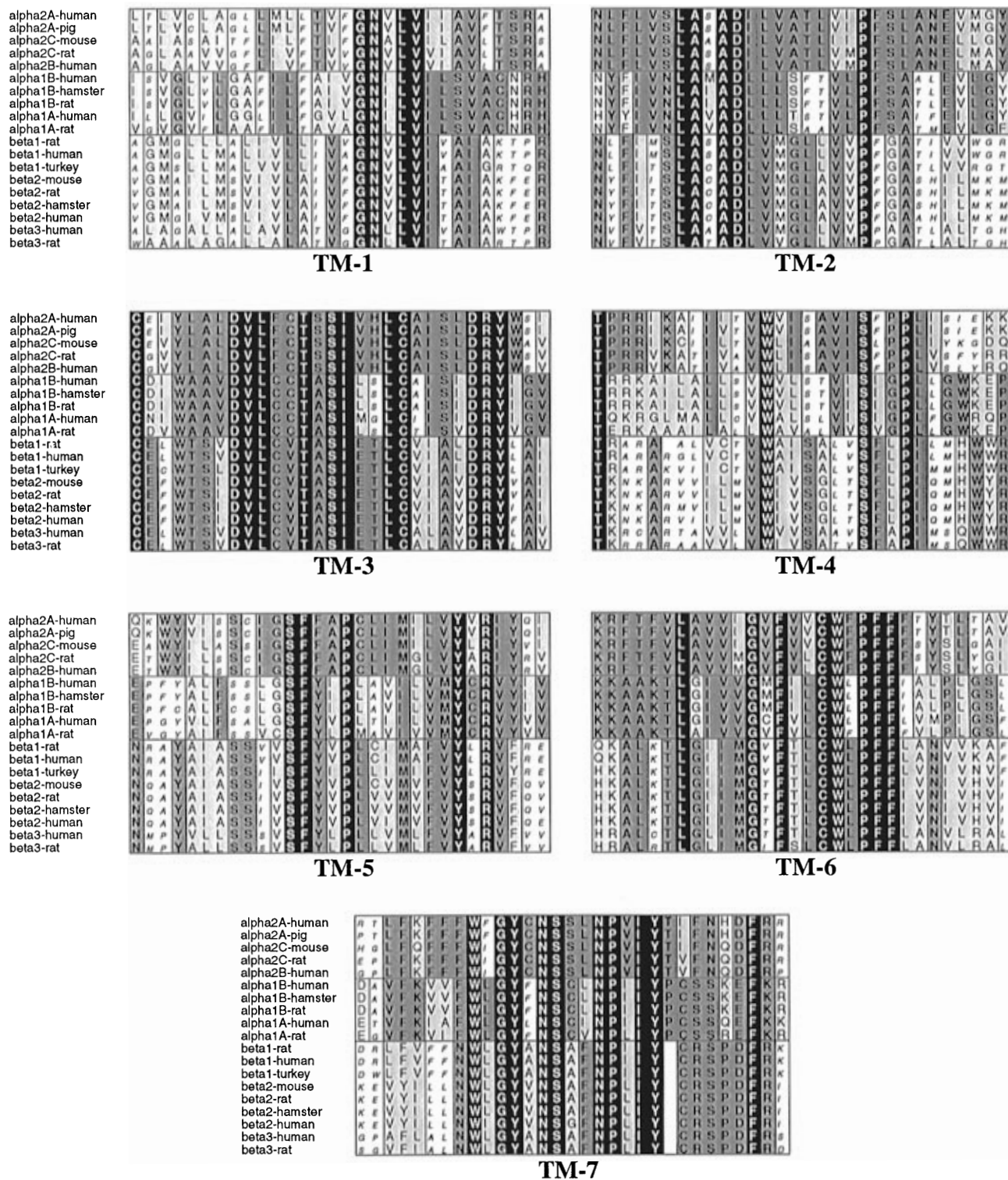


**Figure 16.** Multiple-sequence alignments for the predicted transmembrane regions (TM-1–TM-7) of representative  $\alpha_2$ ,  $\alpha_1$ , and  $\beta$  adrenergic receptors. Blackened blocks indicate positions conserved in all receptors shown in this alignment, dark gray blocks highlight positions conserved within a receptor group (e.g.,  $\alpha_2$  or  $\alpha_1$  receptors), and light gray blocks signify positions where conservative substitutions are observed. This figure was generated with Alscript 2.0.<sup>55</sup>

sequence variation from one receptor subtype to another, in the adrenergic receptor family and in other receptor families we have analyzed, including histaminergic, dopaminergic, serotonergic, and even opioid receptor families. Each of these positions is also localized in the putative ligand binding pocket in our clockwise receptor model. We believe these systematic sequence pattern variations at specific locations in the helix bundle may provide a qualitative structural explanation for receptor

subtype ligand selectivities in the adrenergic receptor family, and possibly in other GPCR families as well.<sup>37</sup>

While static model construction can be quite enlightening, our limited molecular dynamics (MD) studies for a few ligand–receptor complexes with lipid bilayer environments have provided additional information not easily inferred from static models.<sup>28</sup> Of most interest is a proposed Asp–Asn interaction in the helix bundle. After limited MD simulations of epinephrine–receptor

complexes with several different simulation protocols, we observed that Asp-79 from helix 2 is well positioned to form hydrogen bond interactions with Asn-322 from helix 7 in the clockwise model, as shown in Figure 5 (this interaction was not present in our original static models). These two residues are highly conserved in the GPCR family, but multiple-sequence alignments reveal an interesting swap (D79N and N322D) of these residues in a few receptors, such as gonadotropin releasing hormone (GnRH) receptor from various mammalian species. Recently, Sealfon and co-workers mutated these two residues in mouse GnRH receptor to probe this possible interaction.<sup>38</sup> When either residue is mutated independently (D79N or N322D), the receptor is unable to bind hormone or antagonists. When both residues are mutated simultaneously, i.e., "swapped" for each other, the double-mutant receptor binds both hormone and antagonists with essentially wild-type affinity (G-protein-coupling efficiency was diminished somewhat for the double-mutant versus the wild-type receptor, however). Comparable results have been observed more recently for the 5-HT<sub>2A</sub> receptor,<sup>39</sup> which has significant sequence similarity to  $\beta$  adrenergic receptors. The 5-HT<sub>2A</sub> receptor displays binding affinity for a number of  $\beta_2$  adrenergic ligands, implying considerable similarity in the binding pocket of these two receptors. These experimental results, plus the multiple-sequence alignment data, strongly suggest the Asp-79/Asn-322 interaction is real and significant. While our clockwise model displays a classic Asp-Asn interaction between these two residues, all counterclockwise models we have examined have these two residues well separated and oriented inappropriately for favorable interaction with each other (Figure 15). This putative Asp-Asn pair is the first piece of experimental data not directly related to ligand chirality and binding data that appear to favor our clockwise helix-bundle model over other alternatives. We cannot rule out the possibility that rather different counterclockwise helical bundle arrangements would accommodate this Asp-Asn interaction. However, there are no obvious rearrangements we can make in our counterclockwise models to create this Asp-Asn pair interaction that do not significantly degrade other well-established interactions and distort helices 2 and 7 dramatically.

Some caution must be exercised in interpreting these mutation data for Asp-79 and Asn-322, however. Recent results from Barak and co-workers provide somewhat contradictory, and confusing, data for the  $\beta_2$  receptor. They find that nonconservative substitutions of Asn-322 completely disrupt agonist binding and G-protein coupling, as would be expected if this contact pair is important, but that an N322D mutation improves receptor coupling with no adverse effects on other receptor properties.<sup>40</sup> The analogous Asn to Asp mutation in helix 7 of rat cholecystokinin B receptor had absolutely no effect on ligand binding or G-protein coupling.<sup>41</sup> These observations are radically different from the results seen for GnRH and 5-HT<sub>2A</sub> receptors and strongly suggest that it may not be valid to extrapolate results of point mutation studies from one G-protein-coupled receptor to another, even in the case of two closely related receptors such as 5-HT<sub>2A</sub> and  $\beta_2$  adrenergic receptors.

Recently, a series of  $\alpha_2/\beta_2$  chimeric adrenergic recep-

tors was generated by Kobilka and co-workers to probe specific interactions in these receptors, in an attempt to resolve the topology (i.e., clockwise versus counterclockwise) of the seven-helix bundle.<sup>42</sup> These chimeric receptors probe in particular the interactions of three residues in helix 7 of the  $\beta_2$  receptor: Leu-310, Leu-311, and Asn-312. All three residues are phenylalanine in  $\alpha_2$  receptors (see Figure 16), and earlier experimental studies have suggested specific interactions between Asn-312 and residues in helices 1 and/or 2.<sup>43</sup> The results of these experiments suggest that Asn-312 does indeed interact with residues in helix 1 or 2, while Leu-311 interacts with residues in helices 3 and 6. Helix swapping in these chimeric receptors has no impact on Leu-310, and this residue is assumed to be on the exterior surface of the helix bundle. Kobilka and co-workers concluded that these results are more consistent with a counterclockwise arrangement of the helical bundle. However, our models are not completely consistent with this interpretation. Both our clockwise and counterclockwise models predict that Leu-310 is on the exterior of the helix bundle, as do most other models. However, our clockwise model positions Asn-312 in a favorable orientation to interact with residues from helix 2. In fact, this position is one of our signature residues that vary systematically from one receptor class and subtype to another.<sup>37</sup> Only the data for Leu-311 seem to fit our counterclockwise model somewhat better than the clockwise model. However, the effects of the Leu-311 mutation are compensated only by substitution of two complete helices in these experiments, and we cannot easily predict what other structural changes such a dramatic alteration of the receptor may produce. Because of these uncertainties, we have never used full helix substitution data to either support or rule out any particular model. However, helix-bundle chimeras can suggest additional point mutations that should be explored. For example, it would be quite useful if specific residues could be identified in individual helices that compensate the mutation of Leu-311.

Clearly, there is still not adequate data to provide conclusive support for either a clockwise or a counterclockwise helix-bundle model. Most previous models have assumed a counterclockwise helix-bundle arrangement, either because the models were based directly on a bacteriorhodopsin template or because an evolutionary relationship with bacteriorhodopsin was assumed. As discussed previously, it has been shown that there is no solid basis for either of these assumptions. We must then ask whether it is conceivable that two families of integral membrane proteins (GPCR and halobacterial retinal proteins) could both possess seven-helix-bundle motifs but display different helical bundle topologies, i.e., clockwise versus counterclockwise packing arrangements. There are certainly examples of soluble, globular proteins with similar 3D structural motifs but no obvious sequence homology. For example, a four- $\alpha$ -helix-bundle motif is observed in many globular proteins.<sup>44,45</sup> A number of globular proteins with this motif exhibit similar 3D structures, although there is little or no obvious sequence homology. It is also noteworthy that known four-helix-bundle structures are about evenly split between left- and right-handed structures. While it is not reasonable to make any direct extrapolations, observations such as these for well-characterized

globular proteins suggest that a similar situation is at least feasible for seven-helix-bundle integral membrane receptors, i.e., they may not all be related or even exhibit the same handedness for bundle-packing arrangements.

## Conclusions

The results presented here indicate clearly that reasonable 3D models for ligand- $\beta_2$  receptor complexes can be generated, even when rather stringent model construction criteria are applied. We are especially pleased that we can dock a diverse collection of agonists and antagonists, with little or no adjustment to our original receptor models. It is also quite obvious that these models are still severely underdetermined, as there is insufficient definitive experimental data to resolve differences among various proposed models. Perhaps the most dramatic example of the underdetermined nature of these models is the inability to select one of the several possibilities for the stereoselective hydrogen-bonding residues in the receptor. As a result, there are at least three general models proposed by various groups to explain stereoselective binding, and each model has attractive features and weaknesses.

Clearly, the experimental data available presently are inadequate to discriminate among the numerous 3D models regarding precise helix-bundle arrangement or receptor stereoselective determinants. It is rather striking that many aspects of all  $\beta_2$  receptor models are quite similar, with the notable exception of the proposed stereoselective hydrogen-bonding residues. Undoubtedly, this is due to the amount and quality of data available from experimental probes of the receptor binding site, which nearly all researchers use to aid in 3D model construction.

The underdetermined nature of these receptor models highlights their primary utility; underdetermined facets of the models indicate exactly where experimental effort should be focused. As new data are generated, the models can then be corrected and refined to yield better approximations to the true structure. The models can also be used to suggest which techniques may be suited to probe poorly characterized regions of the receptor protein. For example, our relaxed clockwise models indicate that Tyr-316 from the seventh transmembrane helix might function as the stereoselective hydrogen bond partner for  $\beta$  adrenergic ligands. This residue has been mutated previously to alanine. However, this is not a particularly conservative mutation and may well disrupt side chain packing appreciably in that region of the receptor. It would be quite interesting to test a tyrosine to phenylalanine mutation at position 316. This mutation should have minimal effects on receptor structure but noticeable impact on ligand binding and stereoisomer discrimination, if indeed Tyr-316 functions as the key stereoselective determinant.

As we have seen frequently in our model construction exercises, some techniques such as site-directed mutagenesis will often yield rather ambiguous data, especially when general 3D structural models are as uncertain as these.<sup>21</sup> Recent studies have also shown that mutations at supposedly homologous positions sometimes yield quite different results in different GPCR, so extreme caution must be exercised when extrapolating results between GPCR. Furthermore, much site-

directed mutagenesis work to probe the ligand binding site yields data of marginal utility in model construction. For example, when mutation of a proposed key hydrogen-bonding residue alters ligand binding and/or stereoselectivity by only a factor of 2–5, it can be dangerous to assume that these data reflect a direct, specific interaction between the mutated residue and ligand. Unfortunately, many mutated residues yield ligand-binding effects of this magnitude, so there are still many fine details of ligand-receptor interactions that we cannot yet deduce from the experimental data and our modeling exercises. Clearly, detailed biophysical studies for multiple GPCR are needed to provide unambiguous structural information for these receptors. Photoaffinity labeling and cross-linking methods, spin label incorporation for EPR studies, and solid-state NMR spectroscopic techniques can all yield detailed structural data that will facilitate construction and refinement of better 3D models for GPCR. It may well prove impossible to characterize many structural features of these receptors with anything less than high-resolution X-ray diffraction structures for a variety of GPCR. Since high-resolution structures for even a few GPCR are not likely soon, modeling studies coupled with biophysical structural probes will be needed to advance our understanding of these important receptors.

## Experimental Section

Low-energy conformers of each ligand were docked manually in the  $\beta_2$  receptor models generated previously<sup>9</sup> and in an alternate counterclockwise helix-bundle model using interactive molecular graphics modeling techniques. For each complex, key ligand-receptor contacts inferred from experimental studies were maintained (e.g., protonated amine/Asp-113 counterion interactions, hydrogen bonds, etc.). We made an initial assumption that most or all agonists share a similar binding motif, which seems reasonable given their structural similarity and the available structure-activity relationship data. Multiple-sequence alignment data for an assortment of  $\alpha$  and  $\beta$  adrenergic receptors, used previously to aid in construction of 3D receptor models, were employed to identify additional residues that might be involved in direct ligand interactions. Adjustments to the receptor to accommodate any particular ligand were restricted to isolated amino acid side chain rotations in the binding site region, and rotations were further restricted to allowable rotamers tabulated for protein side chains by Ponder and Richards.<sup>46</sup>

Low-energy conformers for each ligand were generated using a systematic conformational search strategy. All rotatable bonds were varied systematically in 30° increments, and all conformers with impossible steric clashes were eliminated. Conformers with energies greater than 10 kcal/mol above the global minimum energy located in the search were also eliminated. All remaining conformers were minimized with torsion constraints on the rotatable bonds. Conformers for subsequent docking exercises were then chosen from the subset of conformers within 3–5 kcal/mol of the "global" minimum structure. For a few of the smaller ligands, we also performed semiempirical (AM1) and/or *ab initio* (3-21G) quantum mechanical calculations (single-point and full geometry optimizations) to verify that the lowest-energy conformers had indeed been selected in the systematic search procedure.

After manual docking, limited energy minimization and MD were used to relieve any residual bad steric contacts. The entire receptor-ligand complex was allowed to move during refinement. Explicit waters were not included in the minimization or dynamics calculations. However, for some of the dynamics calculations, explicit lipid bilayer models and a continuum aqueous solvent model were included.<sup>28</sup> The final docked complexes were examined to insure that receptor models still possessed sensible side chain conformations and

packing interactions as described previously.<sup>9</sup> The quality of ligand–receptor interactions was assessed for steric, charge–charge, and hydrogen-bonding interactions. Hydrogen bonds were considered “good” if donor–acceptor distances were  $\sim 2.8$ – $3.2$  Å and donor–hydrogen–acceptor angles were  $\sim 0.0 \pm 20^\circ$ . As reported previously, a few selected ligand complexes were also studied with MD simulations using several receptor–ligand–bilayer models and protocols.<sup>28</sup> As a further test of our manual ligand docking protocol, we also used an automated docking procedure to probe probable binding site orientations for a few ligands.<sup>35</sup>

Standard AMBER all-atom potential functions were used for all minimization and MD calculations.<sup>47</sup> Partial charges for all ligands were derived from *ab initio* electrostatic potential calculations with Gaussian 90<sup>48</sup> using a 3-21G basis set. The final partial charges were fitted using the CHELPG program.<sup>49</sup> Systematic conformational searches were performed with InsightII.<sup>50</sup> Multiple-sequence alignment and analyses were performed with the AMPS and AMAS programs.<sup>51</sup> Manual docking and visual analysis of complexes were performed using PSSHOW and MD-DISPLAY programs.<sup>52,53</sup> The DOCK package was used for all automated docking exercises.<sup>34</sup>

**Acknowledgment.** Work described here was supported in part by grants from the National Institutes of Health (NS-33290), the National Science Foundation (DMB-9196006), the Searle Scholars Program/Chicago Community Trust, and the Whitaker Foundation.

## References

- Lameh, J.; Cone, R. I.; Maeda, S.; Philip, M.; Corbani, M.; Nadasdi, L.; Ramachandran, J.; Smith, G. M.; Sadée, W. Structure and Function of G Protein Coupled Receptors. *Pharm. Res.* **1990**, *7*, 1213–1221.
- Bockaert, J. G Proteins and G Protein-coupled Receptors: Structure, Function, and Interactions. *Curr. Opin. Neurobiol.* **1991**, *1*, 32–42.
- Savarese, T. M.; Fraser, C. M. In Vitro Mutagenesis and the Search for Structure-function Relationships Among G Protein-coupled Receptors. *Biochem. J.* **1992**, *283*, 1–19.
- Kobilka, B. Adrenergic Receptors as Models for G Protein-coupled Receptors. *Annu. Rev. Neurosci.* **1992**, *15*, 87–114.
- Findlay, J.; Eliopoulos, E. Three-dimensional Modeling of G Protein-linked Receptors. *Trends Pharmacol. Sci.* **1990**, *11*, 492–499.
- Dahl, S. G.; Edvardsen, Ø.; Sylte, I. Molecular Dynamics of Dopamine at the D<sub>2</sub> receptor. *Proc. Natl. Acad. Sci. U.S.A.* **1991**, *88*, 8111–8115.
- Edvardsen, Ø.; Sylte, I.; Dahl, S. G. Molecular Dynamics of Serotonin and Ritanserin Interacting with the 5-HT<sub>2</sub> Receptor. *Mol. Brain Res.* **1992**, *14*, 166–178.
- Lewell, X. Q. A Model of the Adrenergic Beta-2 Receptor and Binding Sites for Agonist and Antagonist. *Drug Des. Discovery* **1992**, *9*, 29–48.
- MaloneyHuss, K.; Lybrand, T. P. Three-dimensional Structure for the  $\beta_2$  Adrenergic Receptor Protein Based on Computer Modeling Studies. *J. Mol. Biol.* **1992**, *225*, 859–871.
- IJzerman, A. P.; van Galen, P. J. M.; Jacobson, K. A. Molecular Modeling of Adenosine Receptors. I. The Ligand Binding Site on the A<sub>1</sub> Receptor. *Drug Des. Discovery* **1992**, *9*, 49–67.
- Trump-Kallmeyer, S.; Hoklack, J.; Bruinvels, A.; Hibert, M. Modeling of G-Protein-Coupled Receptors: Application to Dopamine, Adrenaline, Serotonin, Acetylcholine, and Mammalian Opsin Receptors. *J. Med. Chem.* **1992**, *35*, 3448–3462.
- Yamamoto, Y.; Kamiya, K.; Terao, S. Modeling of Human Thromboxane A<sub>2</sub> Receptor and Analysis of the Ligand-Receptor Interaction. *J. Med. Chem.* **1993**, *36*, 820–825.
- Nordvall, G.; Hacksell, U. Binding-Site Modeling of the Muscarinic m1 Receptor: A Combination of Homology-Based and Indirect Approaches. *J. Med. Chem.* **1993**, *36*, 967–976.
- Cronet, P.; Sander, C.; Vriend, G. Modeling of Transmembrane Seven Helix Bundles. *Protein Eng.* **1993**, *6*, 59–64.
- Zhang, D.; Weinstein, H. Signal Transduction by a 5-HT<sub>2</sub> Receptor: A Mechanistic Hypothesis from Molecular Dynamics Simulations of the Three-Dimensional Model of the Receptor Complexes to Ligands. *J. Med. Chem.* **1993**, *36*, 934–938.
- Donnelly, D.; Findlay, J. B. C.; Blundell, T. L. The Evolution and Structure of Aminergic G Protein-coupled Receptors. *Recept. Channels* **1994**, *2*, 61–78.
- Terlaak, A. M.; Timmerman, H.; Leurs, R.; Nederkoorn, P. H. J.; Smit, M. J.; Denkelder, G. M. D. O. Modelling and Mutation Studies on the Histamine H-1-Receptor Agonist Binding Site Reveal Different Binding Modes for H-1-Agonists-Asp(116)(TM3) Has a Constitutive Role in Receptor Stimulation. *J. Comput.-Aided Mol. Des.* **1995**, *9*, 319–330.
- Henderson, R.; Baldwin, J. M.; Ceska, T. A.; Zemlin, F.; Beckmann, E.; Downing, K. H. Model for the Structure of Bacteriorhodopsin Based on High-resolution Electron Cryo-microscopy. *J. Mol. Biol.* **1990**, *213*, 899–929.
- Herzyk, P.; Hubbard, R. E. Automated Method for Modeling Seven-Helix Transmembrane Receptors from Experimental Data. *Biophys. J.* **1995**, *69*, 2419–2442.
- Pardo, L.; Ballesteros, J. A.; Osman, R.; Weinstein, H. On the Use of the Transmembrane Domain of Bacteriorhodopsin as a Template for Modeling the Three-dimensional Structure of Guanine Nucleotide-binding Regulatory Protein-coupled Receptors. *Proc. Natl. Acad. Sci. USA* **1992**, *89*, 4009–4012.
- Lybrand, T. P. Three-dimensional Models for  $\beta$ -Adrenoceptor-ligand Complexes. In *Membrane Protein Models*, Findlay, J., Ed.; BIOS Scientific Publishers, Ltd.: Oxford, 1995; pp 145–159.
- Taylor, E. W.; Agarwal, A. Sequence Homology Between Bacteriorhodopsin and G-protein Coupled Receptors: Exon Shuffling or Evolution by Duplication? *FEBS Lett.* **1993**, *325*, 161–166.
- Soppa, J. Two hypotheses - one answer: Sequence comparison does not support an evolutionary link between halobacterial retinal proteins including bacteriorhodopsin and eukaryotic G-protein-coupled receptors. *FEBS Lett.* **1994**, *342*, 7–11.
- Unger, V. M.; Schertler, G. F. X. Low Resolution Structure of Bovine Rhodopsin Determined by Electron Cryo-Microscopy. *Biophys. J.* **1995**, *68*, 1776–1786.
- Schertler, G. F. X.; Hargrave, P. A. Projection Structure of Frog Rhodopsin in Two Crystal Forms. *Proc. Natl. Acad. Sci. U.S.A.* **1995**, *92*, 11578–11582.
- Kontoyianni, M.; Lybrand, T. P. Three-dimensional Models for Integral Membrane Proteins: Possibilities and Pitfalls. *Perspect. Drug Discovery Des.* **1993**, *1*, 291–300.
- Wang, H.-y.; Lipfert, L.; Malbon, C. C.; Bahouth, S. Site-directed antibodies define the topography of the  $\beta$ -adrenergic receptor. *J. Biol. Chem.* **1989**, *264*, 14424–14431.
- Kontoyianni, M.; Lybrand, T. P. Computer Modeling Studies of G Protein Coupled Receptors. *Med. Chem. Res.* **1993**, *3*, 407–418.
- Dixon, R. A. F.; Sigal, I. S.; Strader, C. D. Structure-function Analysis of the  $\beta$ -adrenergic Receptor. *Cold Spring Harbor Symp. Quant. Biol.* **1988**, *53*, 487–497.
- Strader, C. D.; Candelore, M. R.; Hill, W. S.; Sigal, I. S.; Dixon, R. A. F. Identification of Two Serine Residues Involved in Agonist Activation of the  $\beta$ -Adrenergic Receptor. *J. Biol. Chem.* **1989**, *264*, 13572–13578.
- Strader, C. D.; Sigal, I. S.; Register, R. B.; Candelore, M. R.; Rands, E.; Dixon, R. A. F. Identification of Residues Required for Ligand Binding to the  $\beta$ -Adrenergic Receptor. *Proc. Natl. Acad. Sci. U.S.A.* **1987**, *84*, 4384–4388.
- Marshall, G. Computer-aided Drug Design. *Annu. Rev. Pharmacol. Toxicol.* **1987**, *27*, 193–213.
- Dohlman, H. G.; Caron, M. G.; Strader, C. D.; Amlaiky, N.; Lefkowitz, R. J. Identification and Sequence of a Binding Site Peptide of the  $\beta_2$ -adrenergic Receptor. *Biochemistry* **1988**, *27*, 1813–1817.
- Meng, E. C.; Soichet, B. M.; Kuntz, I. D. Automated Docking with Grid-based Energy Evaluation. *J. Comput. Chem.* **1992**, *13*, 505–524.
- Kontoyianni, M.; Meng, E. C.; Lybrand, T. P. A comparison of automatic and manual docking methods for  $\beta_2$  adrenergic receptor-ligand complexes. *Proc. 7th Panhellenic Pharm. Conf.* **1994**, 230–235.
- Green, S. A.; Cole, G.; Jacinto, M.; Innis, M.; Liggett, S. B. A Polymorphism of the Human  $\beta_2$ -Adrenergic Receptor within the Fourth Transmembrane Domain Alters Ligand Binding and Functional Properties of the Receptor. *J. Biol. Chem.* **1993**, *268*, 23116–23121.
- M. Stouffer and T. P. Lybrand, manuscript in preparation.
- Zhou, W.; Flanagan, C.; Ballesteros, J. A.; Konvicka, K.; Davidson, J. S.; Weinstein, H.; Millar, R. P.; Sealfon, S. C. A Reciprocal Mutation Supports Helix 2 and Helix 7 Proximity in the Gonadotropin-Releasing Hormone Receptor. *Mol. Pharmacol.* **1994**, *45*, 165–170.
- Sealfon, S. C.; Chi, L.; Ebersole, B. J.; Rodic, V.; Zhang, D.; Ballesteros, J. A.; Weinstein, H. Related Contribution of Specific Helix 2 and 7 Residues to Conformational Activation of the Serotonin 5-HT<sub>2A</sub> Receptor. *J. Biol. Chem.* **1995**, *270*, 16683–16688.
- Barak, L. S.; Menard, L.; Ferguson, S. S. G.; Colapietro, A. M.; Caron, M. G. The Conserved Seven-transmembrane Sequence NP(X)(2,3)Y of the G-Protein-Coupled Receptor Superfamily Regulates Multiple Properties of the Beta(2)-Adrenergic Receptor. *Biochemistry* **1995**, *34*, 15407–15414.

- (41) Jagerschmidt, A.; Guillaume, N.; Goudreau, N.; Maigret, B.; Roques, B. P. Mutation of Asp100 in the Second Transmembrane Domain of the Cholecystokinin B Receptor Increases Antagonist Binding and Reduces Signal Transduction. *Mol. Pharmacol.* **1995**, *48*, 783–789.
- (42) Mizobe, T.; Maze, M.; Lam, V.; Suryanarayana, S.; Kobilka, B. K. Arrangement of Transmembrane Domains in Adrenergic Receptors. Similarity to Bacteriorhodopsin. *J. Biol. Chem.* **1996**, *271*, 2387–2389.
- (43) Suryanarayana, S.; von Zastrow, M.; Kobilka, B. K. Identification of Intramolecular Interactions in Adrenergic Receptors. *J. Biol. Chem.* **1992**, *267*, 21991–21994.
- (44) Presnell, S. R.; Cohen, F. E. Topological Distribution of Four- $\alpha$ -helix Bundles. *Proc. Natl. Acad. Sci. U.S.A.* **1989**, *86*, 6592–6596.
- (45) Harris, N. L.; Presnell, S. R.; Cohen, F. E. Four Helix Bundle Diversity in Globular Proteins. *J. Mol. Biol.* **1994**, *236*, 1356–1368.
- (46) Ponder, J. W.; Richards, F. M. Tertiary Templates for Proteins; Use of Packing Criteria in the Enumeration of Allowed Sequences for Different Structural Classes. *J. Mol. Biol.* **1987**, *193*, 775–791.
- (47) Weiner, S. J.; Kollman, P. A.; Nguyen, D. T.; Case, D. A. An all-atom force field for simulations of proteins and nucleic acids. *J. Comput. Chem.* **1986**, *7*, 230–252.
- (48) Frisch, M. J.; Head-Gordon, M.; Trucks, G. W.; Foresman, J. B.; Schlegel, H. B.; Raghavachari, K.; Robb, M.; Binkley, J. S.; Gonzalez, C.; Defrees, D. J.; Fox, D. J.; Whiteside, R. A.; Seeger, R.; Melius, C. F.; Baker, J.; Martin, R. L.; Kahn, L. R.; Stewart, J. J. P.; Topiol, S.; Pople, J. A. *Gaussian 90*, Revision F; Gaussian, Inc.: Pittsburgh, PA, 1990.
- (49) Breneman, C. M.; Wiberg, K. B. Determining Atom-centered Monopoles from Molecular Electrostatic Potentials. The Need for High Sampling Density in Formamide Conformational Analysis. *J. Comput. Chem.* **1990**, *11*, 361–303.
- (50) InsightII, Biosym Technologies, San Diego, CA.
- (51) Livingstone, C. D.; Barton, G. J. Protein Sequence Alignments: A Strategy for the Hierarchical Analysis of Residue Conservation. *CABIOS* **1993**, *9*, 745–756.
- (52) Swanson, E. *PSSHOW: Silicon Graphics 4D version*; Silicon Graphics: Seattle, WA, 1995.
- (53) Callahan, T. J.; Swanson, E.; Lybrand, T. P. MD Display: An Interactive Graphics Program for Visualization of Molecular Dynamics Trajectories. *J. Mol. Graph.* **1996**, *14*, 39–41.
- (54) Kraulis, P. J. MOLSCRIPT: A Program to Produce both Detailed and Schematic Plots of Protein Structures. *J. Appl. Crystallogr.* **1991**, *24*, 946–950.
- (55) Barton, G. J. ALSRIPT: A Tool to Format Multiple Sequence Alignments. *Protein Eng.* **1993**, *1*, 30–40.

JM960241A